Chapter 3

Methods

Perfect logic and faultless deduction make a pleasant theoretical structure, but it may be right or wrong; The experimenter is the only one to decide, and he is always right.

L.Brillouin, Scientific Uncertainity and Information, 1964

3.1. Experimental

3.1.1. Introduction

This beauty of this experimental set-up was its pristine simplicity. All it consisted of was a single gas train, which culminated in a pearly column of bubbles. It is indeed fascinating to venture into the dynamics of a system as simple and discover and analyze details and patterns so complex. Not only were the results intriguing, the whole ordeal of obtaining the data soon became one of the riveting highlights of this experiment with The BUBBLE Automation WorkBench © (Sarnobat, 2000) for LabVie w ™ and The BUBBLE Chaotic Analysis Toolbox © (Sarnobat, 2000) for MATLAB ™. Screen shots have been provided in the appendix

3.1.2. Set-up Details

A schematic of the experimental apparatus is shown in the **figure 3.1**. The apparatus consisted of a gas flow and metering system, a data acquisition system, a pressure transducer for monitoring the response of the system and a high voltage power

supply for maintaining an electrostatic field between the nozzle and the ground electrode. The high voltage power supply used was Bertan series 225, 0-50kV, regulated high voltage power supply, with remote analog high voltage programming, and remote analog high voltage & current monitoring, via a rear panel connector. The high voltage power supply was interfaced with a PC-based controller through a data acquisition board and, controlled and monitored remotely. A high voltage 'rippler'[1] was built in-house to add a +/- 450 V DC ripple to the output generated by the high voltage power supply. This component was built because of the slow response time (1-4s) of the high voltage power supply to step from high voltage to low voltage. The 'rippler' could respond to control moves at 500Hz.

3.1.2.1. The glass column

A square glass column of 4x4 cm cross-section and 28 cm in height was constructed. The top of the glass column was sealed with a rubber gasket and plexiglass cover fitting with a fitting for attaching an outlet tube. The plexiglass cover was also fitted with a ground electrode through a 1/8-inch Swagelok fitting. The ground electrode was maintained at a depth of 2.5 cm in the glycerin. The value was determined by carrying out various trials with different the electrode

[1] The author acknowledges the creativity of Boyce O. Griffith who was instrumental in the voltage ‘rippler’ being constructed

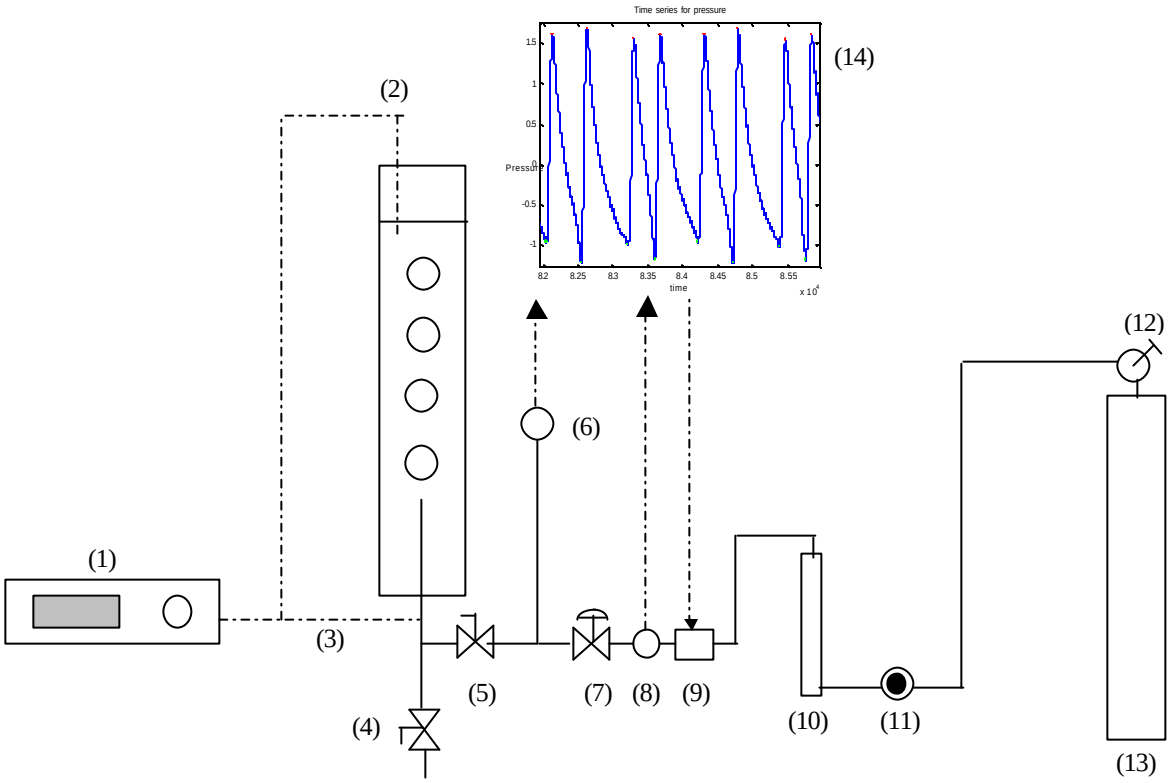

Figure 3.1. Experimental schematic:

(1) High voltage power supply (2) Ground electrode (3) Positive electrode (4) Drain valve (5) Stop valve (6) Pressure transducer (7) Needle valve (8) Flow meter (9) Piezo-electric valve (10) Rotameter (11) Pressure reducer (12) Pressure regulator (13) Nitrogen gas cylinder (14) Data acquisition system

inserted at different depths. It was found that for the trials with a greater surface area of the electrode exposed, the current through the liquid was higher, than it was when a lesser length of the electrode was inserted into the liquid. As a result of the greater current passing through the liquid, the power supply tripped at a lower voltage, thus reducing the range through which the voltage could be varied. With the selected length of the electrode, the power supply could be set to up to 13kV before the current exceeded the hardware limit of 0.3 mA.

Gas was injected into the column through a plastic nozzle with a metal cap orifice, which was electrified with the help of a copper wire passing through the plastic nozzle. The construction of the nozzle is discussed in further detail later in this section. A liquid solution consisting of 99.98% pure glycerin was normally maintained at 8.5 inches above the nozzle.

3.1.2.2.Gas flow and metering system

The type of gas used was chosen so as not to react with the liquid. Nitrogen was found to be satisfactory did not contain significant amounts of moisture. Normal compressed air was not chosen because of the possibility of the liquid absorbing moisture from air, which would then change the conductive properties of liquid. Nitrogen was preferred over dry air because of its property of inertness. The liquid was found to be highly sensitive to moisture and so the column was always kept covered. The gas train used in the characterization experiments, consisted of a pressure regulator, a rotameter, a piezo-electric valve, a flow-meter, a flow control needle valve, a pressure transducer and a stop valve, which were all connected in series. A Brooks' model SHOR-RATE II of tube number R-2-15-D rotameter (6 inch) with stainless steel floats was used for measuring the gas flow rates covering a range of 10-500 cc/min. Since throttling at the control

valve tends to minimize fluctuations in the gas flow-rate upstream of pressure transducer, a fine NUPPO type needle valve located downstream of the rotameter was used to improve gas flow measurement. The key reason for using this needle was to keep the stability of the gas flow constant over the range of investigated flow rates and to minimize the volume between the valve and the nozzle. Without this valve variation of airflow was found at the rotameter due to bubble formation and also the detachment at the nozzle or the damping effect of the gas holdup section. For latter part of the experiments, this was replaced with a MaxTek MV-112 piezo-electric valve with a response time of the 70 microseconds. This valve was interfaced with the DAQ card and accepted a 0-5V, DC. A Cole-Parmer 8168 gas flow meter was used to return the flow rate of both as a digital display signal as well as a 0-5V DC output.

The gas inlet nozzle was equipped with a 0.75-mm internal diameter orifice, which was electrified by a copper wire passing through the nozzle. An elbow in the gas inlet tube prevented liquid buildup in the gas inlet line and residual liquid build-up could be drained periodically using a drain valve. Failure to remove these residual liquids resulted in erratic "burping" of the gas as the bubbles formed at the tip of the nozzle.

A pressure transducer (Setra Systems model 228,having a range from 0 to 1psig) measured the inlet line gas pressure just before the stop valve. The output from the pressure transducer was a 0-5 V DC analog signal, which was fed to the data acquisition board through a signal amplifier, which was set at 10× amplification. The drawback of this transducer was its relatively high time lag (1-3 ms). For latter control part of the experiments, an Endevco piezo-electric pressure transducer (range of 1psig), was used for high accuracy and lower response time (70 micro-seconds). The signal was fed to a National Instruments' SC-2043-SG signal conditioning card, which provided the necessary excitation and was later fed to the data

acquisition card.

3.1.2.3.Liquid selection

Some researchers have shown that the bubbling systems can exhibit chaotic behavior by using low concentrations of glycerin and liquids other than glycerin. Chakka (1994), investigated the influence of liquid density and viscosity on the dynamics of bubble behavior. The results from this experiment suggested that glycerin exhibited the most regular behavior and the clearest apparent bifurcation sequence among three liquids, which were studied (i.e. glycerin, karo syrup and water). Apart from these factors, experiments conducted with electrostatic fields suggested that only glycerin allowed very high voltages to be applied without appreciable current passing through the liquid. Glycerin with an assay of 99.98% (Fisher Chemicals) was chosen. The high voltage power supply used in the experiment allowed a maximum of 0.3mA of current, before the supply tripped. By adjusting the length of the ground electrode immersed in the glycerin, the power supply could withstand a maximum voltage up to 13kV, before the current exceeded the limit and the power supply tripped.

Glycerin was found to be highly sensitive to moisture in the atmosphere. It was also observed that the conductivity of glycerin increased with time, as electric voltage was applied to the liquid. For consistent experimental conditions, fresh glycerin was used for each run, a run being defined as data taken at a constant flow rate, by changing the applied voltage in increments of 1000V from 0V to 10000V, with time intervals of 300s between successive readings, a reading being defined as a snapshot of data being taken for a certain length of time at a constant flow-rate and voltage.

3.1.2.4.Data acquisition system

The data acquisition system consisted of a National Instruments'™ PCI-MIO-16E-50 data acquisition board, (DAQ board) was used with a Pentium™ based PC. National Instruments'™ Labview™ ver. 5.1 was used as the data acquisition software. The DAQ board was configured for differential analog inputs (namely, pressure, current, voltage, output voltage monitor, flow), and differential analog outputs (namely, voltage output to the power supply, piezo-electric valve). The data was taken for 50s at 2000Hz or 5000 Hz, totaling either 100,000 or 250,000 data samples for each reading. For each flow-rate, 11 different voltage settings were used. The data was stored was spreadsheet files which was automatically loaded into MATLAB™ for data processing. The experiment was successfully automated through networking of two computers, with one computer handling the data acquisition and the other computer doing the data analysis as soon as the run was completed. Two separate configurations one each for the simple data acquisition runs and the real time simultaneous AI/AO were used. For the control aspect of the experiment, a LabView *vi*[2] was configured for simultaneous analog input and analog output from 125 Hz to 500 Hz. This aspect of the experiment has been described in detail in a separate report (Sarnobat,2000).

[2]*vi:'virtual instrument', jargon used by National Instruments for routines created with graphical programming interfaces in LabView™.*

3.1.2.5.Nozzle construction

The nozzle was constructed keeping in mind two details (**figure 3.2**):

1) The orifice diameter
2) Chamber size

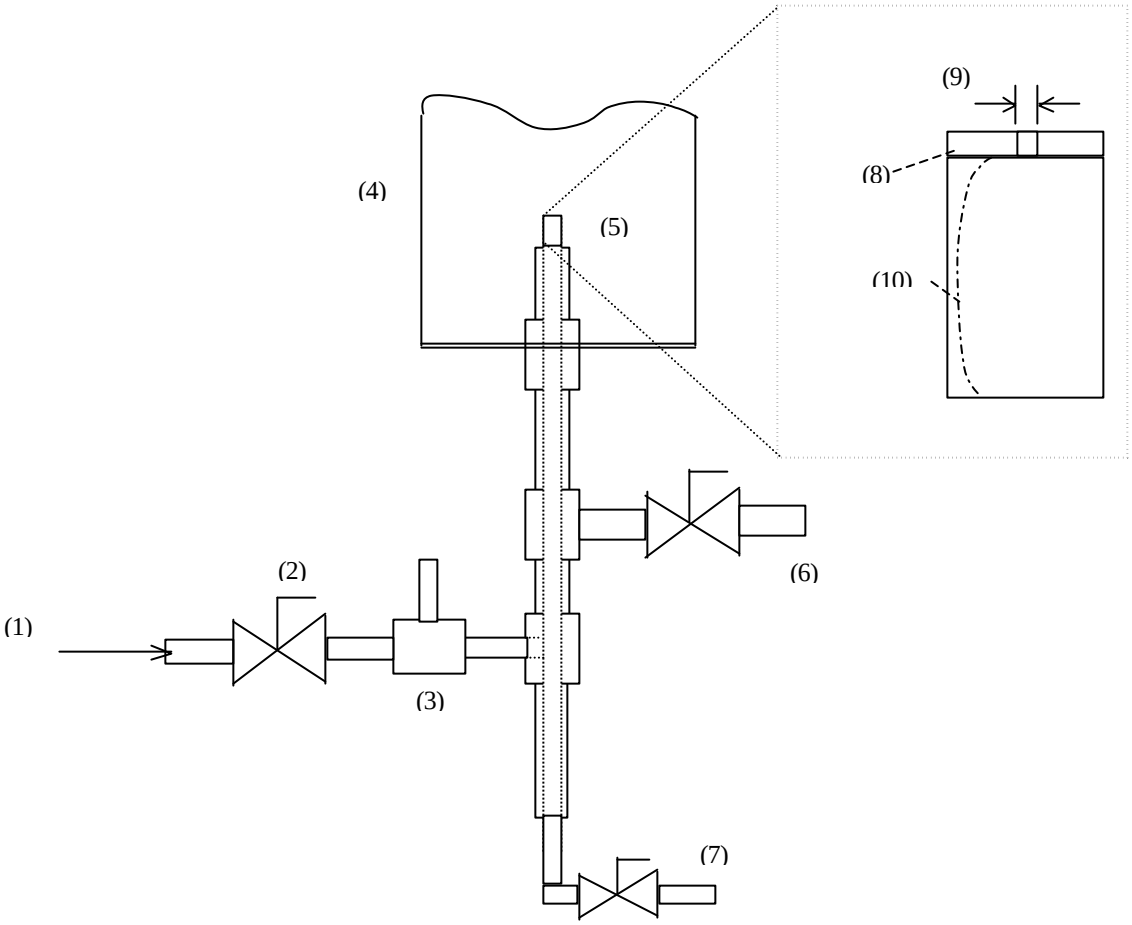

Figure 3.2. Nozzle construction details:

(1) Gas inlet (2) Stop valve (3) Positive electrode connected to nozzle tip (4) Glass column (5) Nozzle tip (6) Column liquid drain (7) Drain for accumulated glycerin (8) Metal cap (9) 0.75mm ID orifice (10) Copper wire

Test runs were carried out in this investigation with a nozzle having a 1mm orifice diameter. The results from this plotted were plotted and rather 'strange-looking' return maps found. So, a slightly smaller orifice diameter & a larger chamber size than previous work (Cheng, 1996) was chosen. This was primarily based on the results obtained from test runs with the 1mm diameter nozzle. It was observed that the glycerin sometimes 'weeped' through the orifice and caused erratic 'burping' of the liquid, causing a renegade spike in the pressure signal. Increasing the chamber volume ensured that the liquid which weeped through could be drained via a tee-bend in the nozzle design.

(The column should be drained prior to switching the gas supply off. In case the glycerin weeps into the gas inlet line, the line should be purged with acetone or methanol and then air/nitrogen keeping the drain open).

3.1.3. Procedure

The experiments were carried out as a series of runs where the flowrate was held constant and the voltage gradually stepped up by increments of 1000V from 0V to 10,000V. The flow rate was varied from lowest permissible flow-rate of a slow period-1, and increased in steps of 5 absolute rotameter units to a highly chaotic bubbling regime . The experiment was automated using LabView and so a large number of runs could be carried out with high efficiency. The automation program varied the voltage, waited for stabilization of the bubbles, which was observed to be less than 300s, checked for instabilities in the high voltage and logged the data acquired as a text file with a record of the date, time, flow and voltage at which the data was recorded at. The rotameter flow rate had to be set manually. The data file contained pressure, voltage and current time series. The data was then preprocessed and variables stored as binary

files, which were later used in conjunction with an indigenously developed, GUI-based MATLAB Bubble Toolbox© to generate various plots for data analysis. The volume of data generated was very large as each run contributed to a data files cumulatively sized at 40MB.

3.2. Data analysis

Various approaches have been adopted for the data analysis of bubbling systems involving chaos. Fractal and deterministic chaos analyses have been adopted to analyze the complex dynamic behavior of multi-phase reactors. Hurst exponents from rescaled-range analysis, various types of fractal dimensions, Kolmogorov entropy and Lyapunov exponents have been used to characterize different hydrodynamic regimes and transitions among them (Kikuchi and co-workers, 1997; Ruzicha, 1997; Leuwisutthichat and coworkers, 1997).

This study was carried out to study the period doubling bifurcation route to chaos with electrostatic fields as the bifurcation variable. The following data analysis techniques were used for the characterization of chaotic bubble behavior.

3.2.1. Power spectra

The classical linear method for analyzing time series was used to transform the information into the frequency domain using Fourier analysis. Fourier analysis proved to be highly sensitive to changes in periodicity of the bubbling system. Femat & co-workers (1998), effectively used power spectra to study periodic-quasiperiodic-chaotic routes. Transitions from one regime to another could be very effectively identified as long as the system was not close to

chaos. When the system went chaotic, the regime could not be predicted conclusively, though it indicated the possibility of chaos. In this study, power spectrum distribution was used to identify the periodicity of bubbling in conjunction with a neural network.

3.2.2. Bifurcation and route to chaos

Bifurcation plots have been widely used in literature (Martien & co-workers, 1985; Mittoni & co-workers, 1994, Tufaile & co-workers, 2000) to illustrate impending chaotic behavior in dynamical systems as a series of changes in the nature of the periodic motions as a result of a variation in some process input variable. For the bubbling process, the changes were quantified in terms of the period of formation of the bubble. Extensive 3-dimensional bifurcation plots were generated to compare and study the simultaneous effect of both electrostatic potential and flow rate on the system.

3.2.3. Time return maps

Time series signals give all the information one needs to observe the dynamics of a system. But the nature of the information can be simplified with the help of time return maps or a Poincare map, without loss of the information about the dynamics of the system. Time return maps were used to transfer all the information of a non-linear time series of pressure measurement and give a visual aid to determine the exact fundamental periodicity of the system. (Moon, 1992). For generating a time return map, a period of formation vector was generated by measuring either the peak-to-peak time distance or the time distance between the troughs.

Another method often cited in literature (Nguyen and co-workers, 1996), is used in conjunction with a zero crossing distance of the waveform. For the control aspect of the experiment, zero-crossings were used with the advantage of faster implementation.

3.2.4. Phase space reconstruction

A classical phase space trajectory plotting of a dynamic system of *N* dependent variables requires *N* dimensions with orthogonal coordinate directions in order to represent each dynamical variable. But, this is limited by the amount of data available for analysis (Takens, 1981). For a system governed by an attractor, the dynamics in the full phase space can be reconstructed from measurements of just one time dependent variable, and this time dependent variable carries sufficient information about all the others (Takens, 1986). Phase space plots were used to conclusively establish the existence of chaos and identify the periodicity of the system.

3.2.5. Multivariate statistical techniques

The periodicity of the bubbling process was modeled using statistical techniques such as regression, principal component analysis, linear and non-linear partial least squares (Sarnobat & Hines, 2000). This was an innovative approach to modeling the bubbling using a data based approach to attempt a numeric model for real time periodicity identification. The input data used was a histogram plot of the period of formation of the bubbles, which was 'regressed' onto a 'regime vector' (**figure 3.3**). The output of the model returned a number (from 1 through 16), which indicated the regime of the bubbling as perio-1, -2, -4 or chaos. Numbers higher than 4 indicated the existence of chaos. Numbers between any two states indicated the extent to which

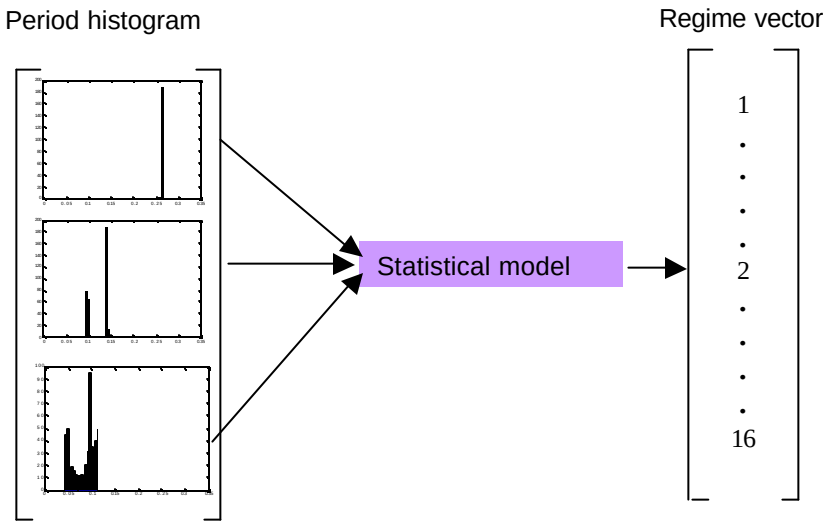

Figure 3.3. Multivariate statistical techniques used to predict the bubbing regime from the period of formation data.

the system corresponded to each regime. The training data used was generated manually by visually inspecting the entire data set for the regime the system was in. Results from this analysis are referenced in a separate paper by Sarnobat & Hines (1999).

3.2.6. Neural network model for regime identification

A neural network model was trained by linear vector quantization (Tsoukalas, L.H, and co-workers, 1997) for identification of the periodicity of the bubbling. Information about the bubbling regimes was extracted by frequency domain analysis using power spectra and identifying fundamental peaks. The fundamental bubbling frequency, (average bubbling frequency), was fed into the neural network along with 5 characteristic peak heights. The neural network used a Kohonen map, (Tsoukalas, L.H, and co-workers, 1997) to cluster the data and the output was the cluster the input belonged to. The network could have discrete outputs of 1,2,4 and chaos. A scheme for real time identification of bubbling periodicity and change in periodicity was identified (**figure 3.4**), (Sarnobat & co-workers, 1999).

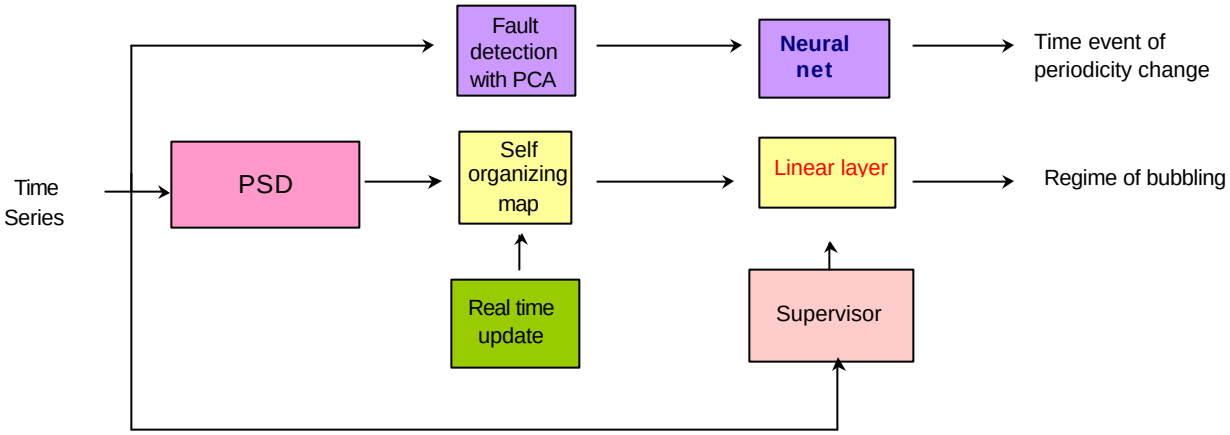

Figure 3.4. Real time identification and fault identification